Physics of the Earth and Planetary Interiors, 7 (1973) 365–378

REGIONAL INDUCTION STUDIES: A REVIEW OF METHODS AND RESULTS

ULRICH SCHMUCKER
Institut für Geophysik, Göttingen (Germany)

Accepted for publication February 2, 1973

The geomagnetic skin-effect is specified by setting three length scales in relation to each other: L_1 for the overhead source. L_2 for the lateral non-uniformity of the subsurface conductor, L_3 for the depth of penetration of a quasi-uniform transient field into this conductor. Relations for the skin-effect of a quasi-uniform source in layered conductors are generalized to include sources of any given geometry by introducing response kernels as functions of frequency and distance. They show that only those non-uniformities of the source which occur within a distance comparable to L_3 from the point of observation are significant. The skin-effect of a quasi-uniform source in a laterally non-uniform earth is expressed by linear transfer functions for the surface impedance and the surface ratio of vertical/ horizontal magnetic variations. In the case of elongated structures and *E*-polarisation of the source, a modified apparent resistivity is defined which as a function of depth and distance gives a first orientation about the internal distribution of conductivity. The skin-effect of a non-uniform source in a non-uniform earth is considered for stationary and "running" sources. Recent observations on the sea floor and on islands indicate a deep-seated change of conductivity at the continent–ocean transition, bringing high conductivity close to the surface, a feature which may not prevail, however, over the full width of the ocean. There is increasingly reliable evidence for high conductivities (0.02 to 0.1 $\Omega^{-1}m^{-1}$) at subcrustal or even at crustal depth beneath certain parts of the continents, in some cases without obvious correlation to geological structure.

1. Introduction

This review is concerned with geomagnetic and magneto-telluric sounding experiments which are performed at a single site or at several sites within a bounded area. Hence, the electromagnetic skin-effect to be studied is produced by eddy currents which do not form closed loops within the boundaries of the surveyed area. They belong to current systems of much larger, usually global dimensions, matching in size those of the inducing external source field.

Even though no exact knowledge may be available about this large-scale induction process, definite conclusions can be drawn about the internal distribution of electrical conductivity from local or regional observations of transient fields. In fact, such studies are indispensable for the investigation of the earth's crust and uppermost mantle which appear to be highly heterogeneous with respect to their conductivity. Global induction studies with slow and deeply penetrating variations proceed from the concept of a radially symmetric earth. Hence, they cannot give more than a mean internal conductivity downward to about 400 km depth as discussed in Rikitake's contribution to this volume.

The review is subdivided into two parts. In the first of these, section 2, I consider methods of data presentation and interpretation, assuming that the data are given in the form of transfer functions in the frequency-distance domain. Typical sets of transfer functions are the impedance tensor, connecting as a function of frequency and location the horizontal components of the electric and magnetic field variations, and the matrix of *W*-coefficients, connecting in a similar way the vertical and horizontal magnetic variations. Banks' and Hermance's contributions to this volume contain details about their actual determination from empirical data.

Section 3 summarizes recent observational results. Review articles on the same topic have been published within the last year by Porath and Dziewonski (1971b), Rikitake (1971), and by Schmucker and

Jankowski (1972). The reader is referred also to extensive bibliographies on this subject, compiled by Fournier (1969) and Barsczus (1970).

2. Methods of data presentation and interpretation

The earth's surface, taken to be flat in regional studies, forms the plane $z = 0$ of rectangular coordinates, z down. All relations are written in M.K.S.-units and refer, if not stated otherwise, to the magnetic and electric vectors of the transient surface field $H = (H_x, H_y, H_z)$ and $E = (E_x, E_y, E_z)$. The field components $H_x, H_y, \ldots$ are to be understood as complex-valued Fourier coefficients with $\exp(i\omega t)$ as a factor in the time domain. We shall assume that the electric vector of the source field is tangential to the earth's surface (TE mode). Inductive response functions of a layered half-space are used for the case of a sinusoidal TE source field with $\exp[i(k_x x + k_y y)]$ as a common factor of all Fourier coefficients in planes z = constant (cf. Weaver's contribution to this volume). If $k = \sqrt{k_x^2 + k_y^2}$ denotes the absolute value of the tangential "wave number" vector $\boldsymbol{k} = (k_x, k_y)$, these response functions are the impedance $Z(\omega, k)$, the inductive scale length $C(\omega, k)$, and the ratio of internal to external parts $S(\omega, k)$ of the magnetic surface field. They are interrelated as:

$$Z = i\omega\mu_0 C \tag{1}$$

$$S = (1 - kC)/(1 + kC)$$

The conversion into the equivalent apparent resistivity of a uniform half-space is given by:

$$\rho_a = \omega\mu_0 |C|^2 \tag{2}$$

when only the moduli of the response function Z and C are to be considered at a certain frequency. An alternative conversion into the depth of a perfect substitute conductor:

$$z^* = \mathrm{Re}\{C\} \tag{3a}$$

and a modified apparent resistivity:

$$\rho^*(z^*) = 2\omega\mu_0 (\mathrm{Im}\{C\})^2 \tag{3b}$$

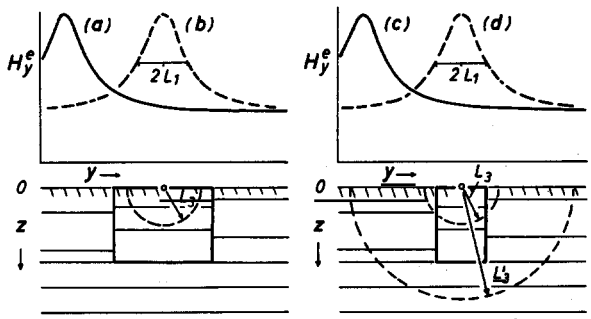

Fig. 1. Horizontal component H_y^e of transient source field for geomagnetic induction in conducting half-space (schematic). Vertical and horizontal boundaries separate uniform blocks. (*a*) and (*b*): One-dimensional skin-effect. (*c*) and (*d*): Disturbed skin-effect. L_1 and L_3: Length scales for source field and depth of penetration at a given frequency.

for this depth takes also their arguments into account (Schmucker, 1970a; p. 69).

The general induction problem as seen from observations at one particular surface point will be indicated by specifying three length scales relative to each other. They refer to the spatial configuration of the source field, to the degree of lateral uniformity of conducting matter beneath the surface, and to the depth of penetration of the fields into this conductor (Fig. 1).

Let L_1 be the first length scale for the spatial non-uniformity of the *overhead* source field. This can be, for instance, the height of an overhead line-current jet or the reciprocal of the wave number k for a sinusoidal field (see below). If the non-uniformity is mainly in one horizontal direction, say in the direction of y, an appropiate value for L_1 is $|H_y/H_y'|$, where $H_y' = \partial H_y/\partial y$ denotes the local gradient of variations of the horizontal component H_y (cf. eq. 6).

The conducting matter of the lower half-space $z > 0$ is subdivided with vertical boundaries into stratified sections of different conductivity. Then L_2 is defined as the distance between the point of observation and the nearest vertical boundary.

In the special case of sufficiently uniform source fields the real and negative imaginary parts of the inductive scale length can be interpreted as the weighted mean depth of the induced currents in a stratified half-space (Weidelt, 1972; p. 268). Hence, the limiting value of C for $k \to 0$ is a convenient measure for the depth of penetration at a given frequency. We shall use its modulus for the relevant stratified section as

the third scale length and set $L_3 = |C(\omega, 0)|$. Clearly, L_3 will increase with decreasing frequency.

2.1. Quasi-uniform source field and quasi-stratified conductor: $L_1, L_2 \gg L_3$.

This is a one-dimensional induction problem because for the point or area under consideration neither the exact configuration of the source field nor the conductivity in adjacent stratified sections matters (Fig. 1a). Insetting the source field parameter k formally to zero, we obtain the field relations for this so-called Cagniard case (cf. Weaver's contribution):

$$E_x = Z(\omega, 0)H_y \qquad E_y = -Z(\omega, 0)H_x \tag{4}$$

$$H_z = 0 \qquad S(\omega, 0) = 1 \tag{5}$$

When allowance is made for a small sinusoidal modulation of the source field with the constraint that $k \cdot |C(\omega, 0)| = L_3/L_1 \ll 1$, vertical magnetic variations and the ratio of internal to external parts are given approximately by:

$$H_z = \begin{cases} i k_x C(\omega, 0) \cdot H_x \\ i k_y C(\omega, 0) \cdot H_y \end{cases} \qquad S = 1 - 2kC(\omega, 0) \tag{5a}$$

Notice that the cited constraint still justifies the use of the response function C for zero wave number (cf. upper left graph in Fig.3). Differentation of the eqs.4 with respect to x and y leads to:

$$H_z = C(\omega, 0)\,(\partial H_x/\partial x + \partial H_y/\partial y) \tag{6}$$

In the derivation use has been made of the second field equation $\operatorname{curl} \boldsymbol{E} = -i\omega\mu_0 \boldsymbol{H}$, which implies that:

$$\partial E_x/\partial y - \partial E_y/\partial x = i\omega\mu_0 H_z$$

In the quasi-stationary approximation of the first field equation, $\operatorname{curl} \boldsymbol{H} = \sigma_0 \boldsymbol{E}$, we may disregard the horizontal gradients of H_z for any finite subsurface conductivity $\sigma_0 = \sigma(z = +0)$. Hence, we have for the vertical gradients of H_x and H_y the relations $\partial H_y/\partial z = -\sigma_0 E_x$ and $\partial H_x/\partial z = \sigma_0 E_y$. Inserting E_x and E_y from the eqs.4 gives:

$$\partial H_y/\partial z = -\sigma_0 Z(\omega, 0) H_y \qquad \partial H_x/\partial z = -\sigma_0 Z(\omega, 0) H_x \tag{7}$$

Any one of the relations (4) to (7) can be used to derive one-dimensional response functions from observations at a single site or at adjacent sites, if field gradients are to be employed. Bailey's contribution to this volume should be consulted for a discussion of the one-dimensional inverse problem, which arises when a conductivity versus depth distribution is to be fitted to a given set of response values.

Here it may suffice to point out that in the actual situation lateral gradients of σ will limit the frequency range, for which the response may be regarded as one-dimensional. In addition there will be random errors connected with experimentally determined response values. As a consequence of both deficiencies, inverse procedures cannot give more than averaged values of σ over a certain depth range with certain confidence limits attached to them.

An effective test for consistency of experimental data is provided by the application of two or more methods concurrently. The example in Fig. 2 indicates the degree of consistency which we may expect under favorable conditions.

The method of magnetotelluric depth sounding in the form given by eq. 4 has been introduced by Cagniard and Tikhonov. It has found wide application because it is source-field-independent under the constraints considered here.

The method of geomagnetic deep sounding according to eqs.5 requires the use of a properly chosen source field vector $\boldsymbol{k}$. This parameter is readily available only for fields of simple geometry as is the case for S_q- and D_{st} variations. A slight modification will take account of the sphericity of the earth (cf. Schmucker, 1970b; Appendix).

Eq.6 has not been used to any extent so far because existing instruments do not have the resolving power to measure lateral gradients of magnetic horizontal variations with sufficient accuracy over short distances. The first field experiment of this type was carried out by Schmidt (1968) near Niemegk observatory south of Berlin where H_z, however, is highly anomalous because of the closeness of the North German anomaly.

The possibility of undertaking sounding experi-

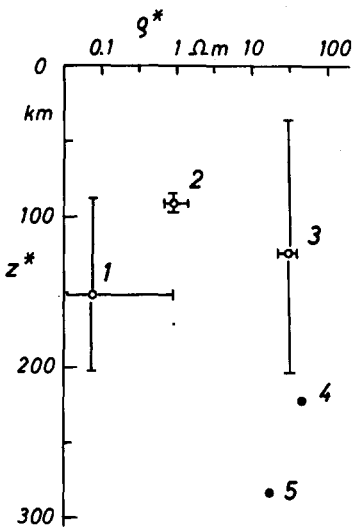

Fig.2. Intercomparison of local sounding data for the third harmonic of S_q variations, given as apparent resistivity ρ^* versus depth estimates (eq.3). *1–3*: Seafloor soundings offshore from California, using the vertical gradient of *D*-variations (*1* and *3*) and the seafloor impedance (*2*). *4* and *5*: Soundings at the nearby inland observatory Tucson, Ariz., using the surface impedance E_{NS}/D (*4*) and the magnetic Z/D ratio. The reduced depth of penetration z^* at the continent–ocean transition implies an increased subcrustal conductivity beneath the ocean. Data from Larsen and Cox (1966) – *1*; Filloux (1967) – *2*; Greenhouse (1972) Station LJG – *3*; Rooney (1935) and Tucson Observatory Yearbook for 1933 – *4*. Calculation of *4* and *5* in S_q-effective coordinates (cf. Schmucker, 1970b, Appendix).

ments with the vertical gradients of H_x and H_y according to eq.7 has been pointed out by Meyer (1966), but again instrumental difficulties have so far prevented any successful application on land – with observations in deep mines or boreholes, for instance. Recently, underwater recording magnetometer stations have become operational and have been installed at the bottom of deep oceans (cf. Filloux's contribution to this volume). Here the high and well-known conductivity of seawater ensures maximum vertical gradients of the horizontal variations. The variations at the sea surface have to be inferred from nearby observations on land (Filloux, 1967; Greenhouse, 1972). The first true gradient observations have been performed in the Arctic Ocean, where Sneyer and Fonarev (1968, 1971) operated simultaneously magnetometer stations on a drifting floe and on the sea floor.

2.2. Non-uniform source field and quasi-stratified conductor: $L_2 \gg L_1, L_3$

Source field dimensions and the depth of penetration are of comparable size ($L_1 \approx L_3$), but the nearest vertical boundary is still far enough away to keep the skin-effect problem one-dimensional (Fig.1b). Hence, in the case of sinusoidal source fields the same relations apply as in section 2.1 except that the response functions Z, C, and S have to be defined now for a finite wave number k. Assuming for simplicity that the source is uniform in the x-direction and thus $E_y = 0$, we obtain:

$$E_x = i\omega\mu_0 C(\omega, k) \cdot H_y = i\omega\mu_0 C(\omega, k)\,[1 + S(\omega, k)]\,H_y^e$$

$$H_z = ik_y C(\omega, k) \cdot H_y \tag{8}$$

$$H_y^i = S(\omega, k) \cdot H_y^e \qquad H_z^i = -S(\omega, k) \cdot H_z^e$$

with $k = |k_y|$. The indices "e" and "i" refer to fields of external and internal origin, respectively. Notice that

$$\left.\begin{aligned} H_z^i &= -i\,\mathrm{sgn}(k_y) \cdot H_y^i \\ H_z^e &= i\,\mathrm{sgn}(k_y) \cdot H_y^e \end{aligned}\right| \tag{9}$$

because both fields are Laplacian for $z \leqslant 0$ with $\exp(+kz)$ and $\exp(-kz)$ as height factors, respectively.

Any given surface field could be decomposed now into a spectrum of sinusoidal undulations to which the eqs.8 or their two-dimensional equivalents are applied individually. This has been done by Hermance and Peltier (1970), Hutton (1972), Hutton and Leggeat (1972), and Oni and Alabi (1972) to evaluate surface observations beneath the equatorial and auroral jet. Their consent was that the choice of the source field parameter is not a critical one because the respective response functions are smooth functions of k for any chosen layered distribution of σ.

The decomposition into spatial harmonics can be circumvented altogether by expressing the relations between field components in the form of convolution integrals. Their kernels as functions of frequency and distance are the Fourier transforms of the response functions for sinusoidal fields above a layered

TABLE I
Response functions and kernels for a stratified conducting half-space

$f(\omega, k_y)$	$F(\omega, y)$ *	$F(y)$ **	$\int_{-\infty}^{+\infty} F(\omega, y)\,dy$
$-i\,\mathrm{sgn}(k_y)$	$K = (\pi y)^{-1}$	–	0
$(ik_yC)^{-1}$	L	$[2h\ \mathrm{tgh}(\pi u)]^{-1}$	0
ik_yC	M	$-[2h\ \sinh(\pi u)]^{-1}$	0
C	N	$\pi^{-1} \cdot \ln[\mathrm{ctgh}(\frac{1}{2}\pi u)]$	$C(\omega, 0)$
S	P	$[2\pi h \cdot (1+u^2)]^{-1}$	1
$(1+S) \cdot C$	Q	$(2\pi)^{-1} \cdot \ln(1+u^{-2})$	$2 \cdot C(\omega, 0)$
$-i\,\mathrm{sgn}(k_y) \cdot S$	R	$[\pi y \cdot (1+u^{-2})]^{-1}$	0

* Cf. eq.10.
** For perfect conductor at the depth h; $u = y/(2h)$

conductor. Physically these kernels represent the inductive response of a layered half-space to a line-current source at zero height (Fig.3).

The required transformation of a wave number response function $f(\omega, k_y)$ is:

$$F(\omega, y) = \frac{1}{2\pi} \int_{\infty}^{\infty} f(\omega, k_y) \cdot \exp(ik_y y)\,dk_y \qquad (10)$$

where $F(\omega, y)$ is the kernel for direct calculations in the distance domain. Details about the numerical evaluation of the integral appearing in eq.10 are given elsewhere (Schmucker, 1971; p.159). Some basic transformation pairs can be found in the first and second columns of Table I.

Apply the convolution theorem to the products on the right hand sides of the eqs.8 and 9, insert the kernel symbols from Table I and obtain:

$$\left.\begin{aligned} &E_x = i\omega\mu_0\{N * H_y\} = i\omega\mu_0\{Q * H_y^e\} \\ &H_z = M * H_y \qquad\qquad H_y = L * H_z \\ &H_y^i = P * H_y^e \qquad\qquad H_z^i = -P * H_z^e = R * H_y^e \end{aligned}\right| \qquad (11)$$

with:

$$H_z^i = K * H_y^i \qquad H_z^e = -K * H_y^e \qquad (12)$$

It should be noted that a convolution with the kernel K is equivalent to the application of the operator K, used by Siebert and Kertz (1957). An extension to two-dimensional fields would involve two successive convolutions. Hobbs and Price (1970, 1971) describe related surface integral methods to separate fields on a spherical surface into two parts of internal and external origin.

Let us choose as an example a simple conductivity model, consisting of a perfect conductor at the depth $z = h$ and zero conductivity for $z \leqslant h$. Its response functions for sinusoidal fields are $C(k) = \mathrm{tgh}(kh)/k$ and $S(k) = \exp(-2kh)$ as is readily verified from the height factors of the internal and external fields which are $\exp(+k\hat{z})$ and $\exp(-k\hat{z})$, respectively; $\hat{z} = z - h \leqslant 0$. These functions are real and naturally the same for all frequencies. Their Fourier transforms can be found analytically and are listed in the third column of Table I. They are shown graphically in Fig. 3.

The most important characteristic of response kernels is their rapid decrease when the distance y

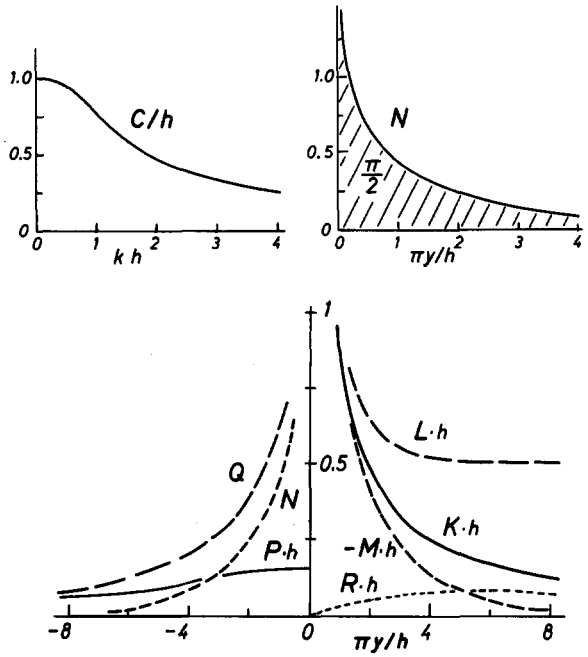

Fig.3. Upper graphs: Response function C and response kernel N, connecting the orthogonal horizontal components of the electric and magnetic surface field above a perfect conductor at the depth $z = h$.
Lower graph: Various response kernels for the same model (cf. eqs.11 and Table I).
Physical interpretation: If the source is a line current at $y = 0$ and $z = -0$, yielding $H_y^e = H_0 \cdot \delta(y/h - 0)$ at $z = 0$ for a current of the strength $2H_0h$ in the negative x-direction, the curves shown represent H_z^e of the source field $(-Kh)$, H_y^i and H_z^i of the internal field (Ph, Rh), and the electric field E_x antiparallel to the current $(i\omega\mu_0 hQ)$, all field components being normalized with respect to H_0.

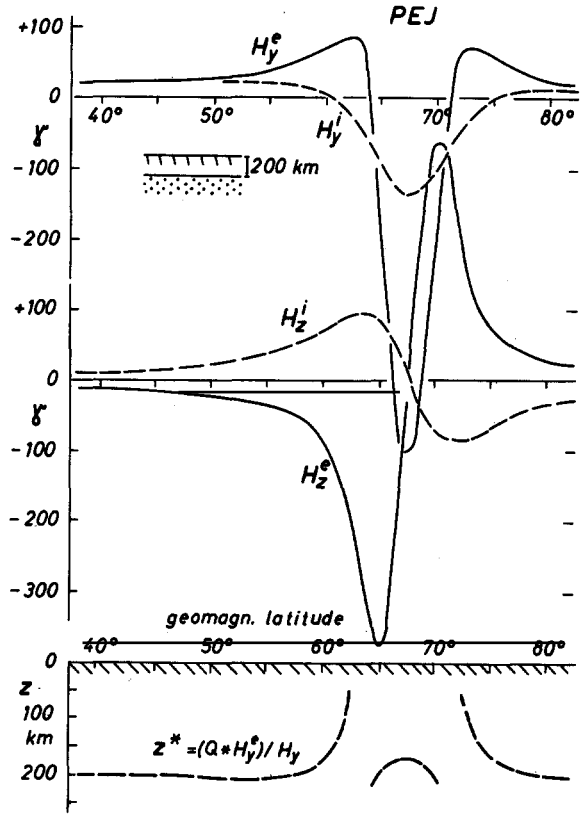

Fig.4. Application of eqs.11 to the idealized two-dimensional field of the polar electrojet (PEJ) during a bay disturbance. Induction takes place in a perfect conductor at 200 km depth. The non-uniformity of the source field produces a clearly reduced and smoothed internal magnetic field. However, the one-dimensional conversion of the local surface impedance into the depth z^* of a perfect substitute conductor recovers the input of 200 km quite well except near to the flanks of the PEJ.

exceeds the depth of penetration for a quasi-uniform source – here the depth h of the perfect conductor. This simply illustrates that the skin-effect at any given surface point does not depend critically on the source field configuration at a distance which is much larger than the relevant length scale L_3. This rule does not apply, however, to the response function L which has $[2C(\omega, 0)]^{-1}$ as the asymptotic value for $y \to \infty$.

Suppose the field component to be convoluted, say H_y, is nearly uniform around a surface point $y = y_0$ up to a distance comparable to $L_3 = |C(\omega, 0)|$. Then the convolution of H_y with a response function F, carried out at this point, may be written approximately as:

$$F * H_y = H_y(y_0) \cdot f(\omega, 0)$$

where $$f(\omega, 0) = \int_{-\infty}^{+\infty} F(\omega, y)\, dy$$

The last identity is readily verified when we express $f(\omega, k_y)$ as an inverse Fourier transform of $F(\omega, y)$ and set $k_y = 0$. Specific values of the integral can be found in the last column of Table I.

The eqs.4 and 5 emerge now as special versions of

the eqs.11 for the limiting case of a nearly uniform surface field, thus clarifying the concept of "quasi-uniformity" in section 2.1.

The response kernels of Fig.3 are applied in Fig.4 to an external field which resembles the surface field of the polar jet along a geomagnetic meridian. The skin-effect is produced by a perfect conductor at 200 km depth. The resulting impedance of the total (external plus internal) surface field is used to derive local estimates of the depth of a perfect substitute conductor along the meridan according to eq.3a. Actually, this substitution should be meaningful only for a quasi-uniform field. We obtain, however, good estimates of the true model depth of 200 km except near the flanks of the polar jet where the horizontal field has its strongest gradients. This again underlines the fact that a non-uniformity of the source field only matters if it occurs within a distance from the point under consideration, which is comparable to the relevant length scale L_3.

The application of the eqs.11 to field data requires that the convolution integrals are approximated by sums, yielding a system of linear equations in accordance with the number of sites at which observations have been made.

Its solution would give the respective response kernel as a function of distance. No serious attempt has been made yet, however, to exploit in this way the non-uniformity of natural source fields for deep sounding at a fixed frequency.

2.3. *Quasi-uniform source and non-uniform conductor:* $L_1 \gg L_2, L_3$

The distance to neighbouring sections with different stratified conductivity is comparable with the depth of penetration. With $L_2 \approx L_3$ this leads to a disturbed skin-effect at the point under consideration, while the source field is regarded as quasi-uniform (Fig.1c). The last constraint allows us to retain the concept of linear transfer functions which, at a given site (x, y) and frequency, connect the various components of the surface field vectors. In analogy to the one-dimensional case (eq.4) the following notations are used:

$$\left.\begin{aligned} E_x &= Z_{xx}H_x + Z_{xy}H_y \\ E_y &= -(Z_{yx}H_x + Z_{yy}H_y) \end{aligned}\right| \quad (13)$$

$$H_z = AH_x + BH_y \quad (14)$$

By letting the effect of neighbouring sections become negligible ($L_3/L_2 \to 0$) the diagonal coefficients Z_{xx} and Z_{yy} disappear, while the off-diagonal coefficients asymptotically approach the one-dimensional impedance $Z(\omega, 0)$.

Eq.14 extends the original concept of *Parkinson-Wiese induction arrows* to complex Fourier coefficients of magnetic variations. The transfer functions A and B for the vertical field should refer, if possible, only to the disturbed skin-effect and not be connected with spatial gradients of the source field. Hence, any source-field-dependent component of H_z should be removed with the aid of eq.5a or 6 before deriving A and B from field observations.

Current numerical methods for the skin-effect of a quasi-uniform source field in laterally non-uniform conductors are reviewed in this volume by Jones. For all practical purposes such calculations are restricted to two-dimensional models, assuming lateral uniformity of σ in one horizontal direction, or to non-uniform thin sheets of variable total conducticity or conductance τ, assuming zero conductivity in the top layer of any underlying stratified conducting medium (cf. Ashour's contribution to this volume).

The interpretation of empirical transfer functions relies at the present time on curve-fitting techniques, carried out on selected profiles perpendicular to the strike of elongated subsurface structures. This special choice of coordinates splits the perturbation of the induced field into two distinct modes: depending on the orientation of the tangential source field vector we can distinguish between E-polarisation (E parallel to the strike) and H-polarisation (H parallel to the strike).

In the first case induced currents do not cross boundaries and flow parallel to the strike in planes z = constant. Hence, any local perturbation of the induced field is also a tangential electric TE field. In the second case induced currents do cross boundaries and there will be up and down going currents near vertical (or sloping) boundaries, generating a tangential magnetic TM perturbation in the induced field. Its magnetic vector is horizontal and parallel to the strike within the conducting half-space and (in quasi-stationary approximation) zero above it. Note that the currents involved are induced in either case in an

unbounded half-space, coming from and going to infinity to form loops of infinite size.

Since no vertical magnetic variations occur in the case of H-polarisation, the transfer functions for the disturbed surface field above a two-dimensional structure may be written as:

$$E_{\parallel} = Z_{\parallel} \cdot H_{\perp}$$
$$E_{\perp} = Z_{\perp} \cdot H_{\parallel} \qquad (13a)$$

$$H_z = A_{\parallel} \cdot H_{\perp} \qquad (14a)$$

The subscripts "$\parallel$" and "$\perp$" refer to orientations parallel and perpendicular to the strike.

Note that $E_{\perp}$ changes discontinuously, wherever vertical (or sloping) boundaries reach the surface because the induced current flow at the subsurface level $z = +0$ must be divergence-free. Hence, $E_{\perp}$ will be determined mainly by near-surface changes of conductivity provided they occur sufficiently close that $L_2 \leqslant L_3$. As a consequence, the impedance for H-polarisation $Z_{\perp}$ may not resemble at all the one-dimensional impedance $Z(\omega, 0)$ for the site under consideration, when L_3 is comparable to or larger than L_2.

The impedance of E-polarisation $Z_{\parallel}$ will do so, however, particularly when at low frequencies the depth of penetration may exceed the scale length of any lateral non-uniformity as shown by the large semi-circle, marked L_3', in Fig.1.

Herein lies the important difference in the behaviour of the electric surface field for E- and H-polarisation (cf. Schmucker and Jankowski, 1972; Fig.5).

The conversion of $Z_{\parallel}$ into apparent resistivity values according to eq.2 or 3 provides a first approximation to the change of true resistivity with depth and distance. This is demonstrated in Fig.5 by means of a simple step model.

Firstly, the magnetic and electric surface fields are found by numerical methods. Then a response function $C_{\parallel} = E_{\parallel}/(i\omega\mu_0 H_{\perp})$ is derived for each surface point y, varying the frequency over several orders of magnitude. Its modulus defines the apparent resistivity ρ_a according to eq.2. Following Madden and Swift (1969), contours of $\rho_a(\omega, y)$ are drawn in a distance-frequency plane, plotting the frequency on a logarithmic vertical scale to simulate the increasing depth of penetration with decreasing frequency. In these contours the general appearance of the orginal step model is already clearly recognizable.

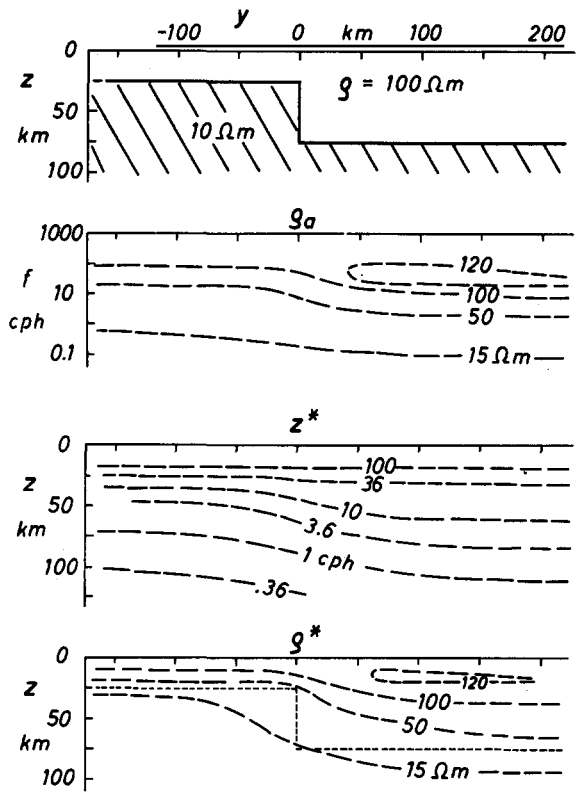

Fig.5. Conversion of calculated transfer functions for a two-dimensional step-model (top) in E-polarisation into apparent resistivities: (1) as a function of frequency f and distance y (ρ_a); (2) as a function of depth z and distance (ρ^*). The input model is recognizable in the contours of ρ_a and ρ^*, thus yielding a first orientation about the true resistivity structure in the case of empirical transfer functions.

In the alternative approach of eq.3, the real part of $C_{\parallel}$ is interpreted as a depth z^*. Curves $z^*(y)$ for ω = constant reflect the changing depth of penetration with distance y into the chosen model. Finally, a modified apparent resistivity ρ^* is derived from $\mathrm{Im}\{C_{\parallel}\}$ for the depth z^* at a given frequency and location. The resulting contours of $\rho^*(z^*, y)$ in the vertical depth-distance plane resemble rather closely a smoothed version of the input model, yielding a good starting distribution for subsequent refined model calculations in the case of empirical transfer functions.

Suppose that lateral non-uniformities may be regarded as being confined to a thin surface layer of variable conductance $\tau(y)$. This conductance can be found directly from a given transfer functions $Z_{\|}$ or $A_{\|}$ for E-polarisation (Schmucker, 1971). Any stratified conductivity distribution beneath this layer enters into the inverse procedure. Hence, if certain constraints can be placed upon acceptable values of $\tau(y)$, a model for the underlying stratified conductor will evolve. In this way well known surface structures can be utilized for a deep sounding experiment (Winter, 1973).

If the surface layer is insulated by a high-resistivity zone from any conducting matter at greater depth, continuity of the sheet current for H-polarisation requires that the product $E_{\perp}\tau$ is constant. Hence, any variability of τ can be inferred directly from the electric field component normal to the trend of elongated structures (Haak, 1970).

2.4. *Non-uniform source field and non-uniform conductor: L_1, L_2, L_3*

The source field dimensions, the size of the laterally uniform sections of the conductor and the depth of penetration are all of comparable magnitude. A general problem of this type is posed, for instance, by the induction of the diurnal variations in large oceans, separated by more or less insulating continents.

As discussed in detail by Ashour in this volume, the problem is treated under the simplifying assumption that oceans and continents form a thin sheet or shell of variable conductance. In order to prevent induced currents from entering or leaving the non-uniform sheet or shell, a perfect insulator is placed between them and any stratified conductor at greater depth. If alternatively a non-uniform layer of finite thickness is considered, source field and conductor must be two-dimensional and uniform in the same horizontal direction to keep the resulting skin-effect problem two-dimensional and thus solvable with existing numerical techniques. It may be noted that in either case with these constraints we have eliminated TM modes from the induced field.

Two examples may illustrate model calculations of the second type. The first example refers to the Andean anomaly in magnetic day-time variations in southern Peru (Fig.6). The chosen non-uniform source field, arising from the equatorial jet, oscillates in-phase along

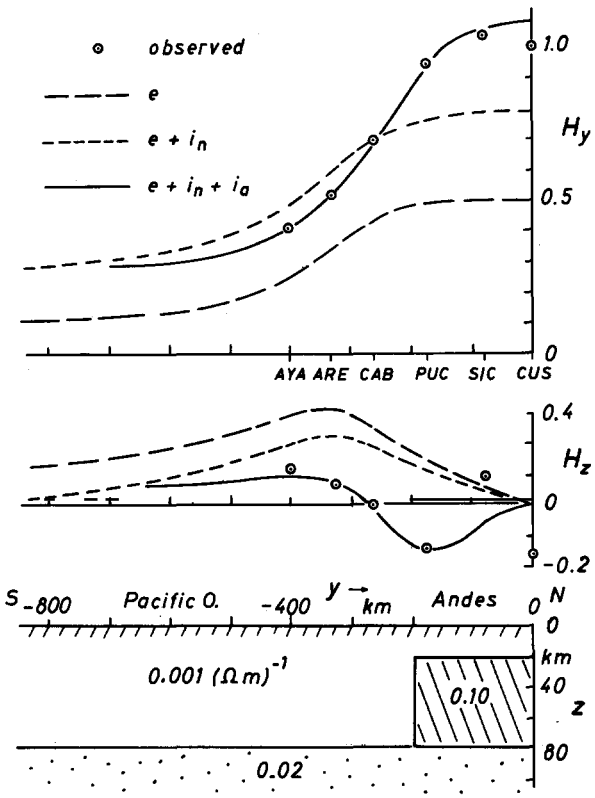

Fig. 6. Geomagnetic induction by the equatorial jet field in southern Peru during day-time events. The chosen source field oscillates in-phase along the profile normal to the dip equator at $y = 0$ with a period of one hour. The induction takes place in a two-layer earth model with a slab of high conductivity under the Andes. e: source field, i_n: internal field without slab, i_a: perturbation of the internal field by the slab. All field components are normalized with respect to H_y at the equator and only their in-phase components are shown. Data points from Schmucker et al. (1964).

the profile with a period of one hour. The induced field is calculated first for the indicated two-layer model, omitting the slab of high conductivity under the Andes and applying the eqs.11 to the source field. Then the perturbation of the induced field due to the high conductivity slab is found by numerical methods and added to the external and undisturbed internal field. The source field and conductivity model have been chosen by trial and error in the best possible way to explain the observed variations equally well during day-time events, when the jet is present, and during night-time events, when the overhead source

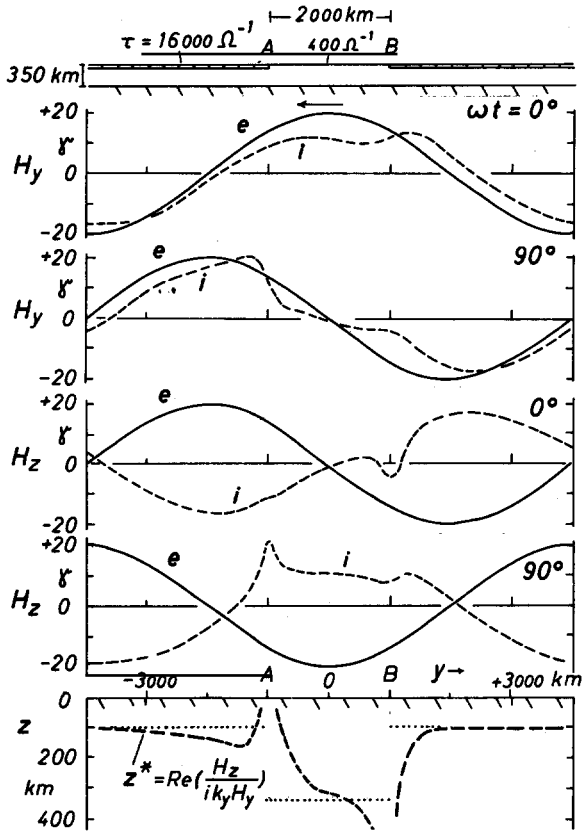

Fig.7. "Running" source field over an ocean with a continental strip AB above a perfect conductor at 350 km depth. τ: conductance of surface sheet. Wave length of the source field and its speed of propagation simulate progression of third harmonic of diurnal variation with local time from east (right) to west (left). Horizontal and vertical components of the external ("e") and internal ("i") field are shown for two instances of time, two hours apart ($\omega = 3 \cdot 360°$/day). Note asymmetry of edge effects at A and B due to the source field progression. The dashed curve in the depth–distance plot at the bottom connects local estimates of the depth of a perfect substitute conductor, derived from the surface ratio of vertical/horizontal variations. They are in good agreement with one-dimensional values of z^* for the oceanic and continental model section (dotted lines) except near to the edge points A and B. Observe the difference in agreement in luff and lee of the continental strip.

from polar disturbances is extremely uniform.

In the second example a sinusoidal source field $H_y^e \sim \exp(ik_y y)$ with a wave length $\lambda = 2\pi/k = 8000$ km moves with 1000 km per hour from the left to the right (Fig.7). Hence, oscillations with a period of 8 hours will be observed at a fixed site. This corresponds to the third harmonic of diurnal variations, progressing with local time from east to west. Its wave length is one fifth of the earth's circumference $2\pi a$ and applies to a spherical surface harmonic of degree $n = 4$, setting $k = (n + 1)/a$.

The conductivity model consists of a thin sheet with a conductance of $16000\,\Omega^{-1}$, representing an ocean of 4 km depth. The sheet is interrupted by a less conducting "continental" strip AB, 2000 km in width. A perfect conductor at 350 km depth simulates high conductivities in the mantle.

The induced surface field for this model has been found by deriving first the current density in the thin sheet (cf. Schmucker, 1971; p.962). Since the source has a well defined wave number, a local estimate of the response function $C(\omega, 0)$ will be obtained according to eq.5a from $C = H_z/(ik_y H_y)$; here H_z and H_y are to be understood as the sums of their respective external and internal parts at a given surface point.

The real part of C is shown as a local estimate of the depth of a perfect substitute conductor. A one-dimensional calculation of z^* would have given 104 km for the ocean and 347 km for the continent. It will be noted that these local estimates which could have been the outcome of a sounding experiment at a single site are fairly close to their one-dimensional values except near to the "coastlines" at A and B.

3. Results

The deeply penetrating D_{st}-recovery phase of magnetic storms appears to have a globally uniform ratio of internal to external parts (Grafe, 1964; table 5). This suggests radial symmetry of conductivity in the deeper parts of the upper mantle.

The internal part of S_q, on the other hand, is affected quite clearly by a regionally changing depth of penetration. This is seen most conspicuously in the diurnal variations of Z (vertical magnetic component). Amplitude and phase of their harmonic coefficients deviate at many observatories from their theoretical values, derived from a global analysis of S_q under the assumption of radial symmetry. The latest analysis of this kind has been published by Parkinson (1971).

"Anomalous" S_q observatories lie almost exclu-

sively near coastlines and on islands. This suggests the influence of strong currents which are induced in the oceans and diverted around continents and islands (cf. Larsen's contribution to this volume). However, when Filloux (1967) made the first magnetic observations on the seafloor offshore from central California, he found a surprisingly small attenuation of the diurnal variations in D(east component). It amounted for the second harmonic to barely 10%, whereas a continental type substructure would have given an attenuation of about 40%. This observation implies a reduced strength of induction currents in the seawater and thus an oceanic substructure which is better conducting than a continental one, to which all other observations have referred so far.

It appears now that Filloux's experiment may have been performed in a locally anomalous situation. Recent seafloor experiments by Greenhouse (1972) in the same general area, but at a slightly larger distance from the continental shelf, have revealed an attenuation of the semi-diurnal harmonic in D of about 30%. Greenhouse finds that his semi-diurnal harmonics in D and Z are explained best by a perfect conductor which rises from 500 km under the continent to 300 km beneath the ocean.

A detailed study of the "island" anomaly of geomagnetic variations on Ohau (Hawaii) has been used by Klein (1972) to estimate the strength and phase of induction currents in the open ocean which are diverted around the islands of Hawaii. His calculations are based on a disturbed flow of steady-state sheet currents. From the known conductivity of seawater Klein has then derived an estimate of the electric field and thereby of the response functions for the Pacific Ocean near Hawaii, finding no evidence for unusually high conductivities at subcrustal depth.

The transition from the continent to the ocean offshore from Nova Scotia has been investigated by Srivastava and White (1971) and by Hyndman and Cochrane (1971). They find the expected enhancement of Z-variations at the coastline, but exceedingly small Z-variations on Sable Island within the continental shelf. The superficial coast effect would have given a much smoother decrease of Z toward the open ocean. The diurnal variations of the total field show also an unusual behaviour at the continent– ocean transition (Srivastava, 1971).

On the basis of two-dimensional model studies Hyndman and Cochrane explain these observations by a crustal layer of high conductivity beneath the shelf, extending from the shore line to the continental slope. Its cause could be a thick layer of sediments. The authors discuss also various alternative explanations, among them the possibility that the conductivity of the lower crust is locally increased by a hydrothermal alteration.

Cox (1971) proposes a similar process for the origin of the shallow layer of high conductivity beneath the ocean offshore from central California. The model which Filloux (1967) derived from magneto-telluric seafloor observations involves resistivities of only a few ohm-meters at 15 to 35 km depth. Cox suggests on the basis of recent laboratory experiments that at this depth serpentinization of ultramafic mantle material takes place, leading to a vastly increased mineral conduction through a fine dust of magnetite and other iron-rich oxides.

The masking of deep continental structures by sedimentary basins has been realized, since magneto-telluric soundings revealed the large conductance which such basins may have. Attention is called in this context to recent sounding experiments by Vozoff (1972) in the Gulf Coast area of Louisiana. He reports sediments with a conductivity above $1\ \Omega^{-1}\ m^{-1}$ throughout a thickness of at least 10 km. Their overall conductance of more than $10^4\ \Omega^{-1}$ is quite comparable to the conductance of deep oceans. Porath and Dziewonski (1971a) therefore suggest that oceanic induction currents enter into the sediments of the Gulf Coast area and produce a displaced "coast effect" at the Ouachita Mountain front in east Texas. It appears that the highly variable Z-amplitude of bay-type disturbances which Moses et al. (1966) report from the southeastern and eastern United States is caused by similar interspersed basins of high conductance.

Porath and Dziewonski (1971b) have classified under these aspects the presently known inland anomalies which cannot arise from mantle sources because of their small half-width. A large group of anomalies is explained solely by sedimentary structures. Among them are the North German anomaly and various distinct anomalies in the Great Plain province of North America.

A second type of anomaly occurs whenever sea channels connect large bodies of water. Porath and

Dziewonski cite as an example the strait of Bonifacio between Corsica and Sardinia.

Anomalies of a third type are connected with the concentration of shallow induction currents in upper crustal lenses of high conductivity as discussed below. A special case is the leakage of oceanic induced currents through continental barriers, separating for instance inland seas from the open ocean. An example is the anomaly in southern Scotland where in the extension of the Firth of Forth a subsurface conducting connexion seems to exist between the Irish Sea and the North Sea (Edwards et al., 1971).

A new analysis of diurnal variations has been completed by Camfield and Gough (1973) for the northwestern United States, using the records of large magnetometer arrays. They find no significant spatial differences in Z-variations at the diurnal periods. This agrees with Caner's (1971) results for western Canada and limits the possible downward extent of high mantle conductivities under the northern Rocky Mountains, which reduces so markedly the Z-amplitude of bay-type disturbances in this region. Hence, the conclusion of Caner et al. (1969) that the difference in deep conductivity between the northern Rocky Mountains and the Great Plain province is con fined to a certain layer at subcrustal or even intracrustal depth now finds additional support. The corresponding conductivity contrast in the southern Rocky Mountains should extend downward, however, to substantial depth because the Z-amplitude of diurnal variations definitely increases at the mountain front, going eastward (Schmucker, 1970a).

Caner (1971) and Caner et al. (1971) have summarized their results, concerning the transition from low-Z regions to high-Z regions in western Canada. Geomagnetic and magneto-telluric observations have been combined in the sense that two concentrated efforts were made to obtain with magneto-telluric soundings the downward change of conductivity, one in the low-Z region and the other in the high-Z region. These soundings provided constraints for the subsequent interpretation of spatial differences in Z.

Caner and his co-authors conclude that beneath the Canadian Rockies a high conductivity layer exists ($\sigma \approx 0.1\ \Omega^{-1}\mathrm{m}^{-1}$) which is absent under the Great Plains. Its upper bound is placed at 15 km depth, whereas its lower bound is ill defined, lying somewhere between 40 and 60 km depth.

Similar crustal or subcrustal layers of high conductivity have been inferred from magneto-telluric soundings at various sites, but apparently in no obvious correlation to known geological structures. Pertinent data have been published by Berdichevskij et al. (1969) for Yakutia, by Adam (1970) for the Carpathian basin, by Hermance and Grillot (1970) for Iceland, by Dowling (1970) for Wisconsin, by Mitchell and Landisman (1971) for Texas, by Oni and Alabi (1972) for Nigeria. Fournier's treatise (1970) should be consulted for further references and a description of his own results, concerning a "couche conductrice intercalaire" beneath western Europe (fig.61). Supporting evidence for the intermittent appearance of high conductivities at shallow depth comes from anomalies of geomagnetic variations with a small spatial half-width, but with no indication of a superficial origin from sedimentary structures. This applies in particular to the Central Plains anomaly in North America (Camfield et al., 1971; Porath et al., 1971) and to an equally pronounced anomaly which has been detected recently on the Ukrainian shield (Rokitjanskij et al., 1969).

In either case we may expect a crustal lens of high conductivity within the otherwise highly resistive crust. This lens must have a conducting connection to a deeper depth range of comparable conductivity and large lateral extent, from which induced currents are drawn into the crustal lens. Similar problems are posed by the Andean anomaly in southern Peru and by the Alert anomaly on Ellesmere Island in the Canadian Arctic (Niblett and Witham, 1970). The former is explained best by a subcrustal channel of high conductivity, following the trend of the Andes (Fig.6).

A first attempt to utilize a well known sedimentary structure for geomagnetic soundings (cf. section 2.3) has been carried out in the Rhine graben area by Winter (1973). Resistivity measurements in bore holes and telluric observations by Haak (1970) allow a fair estimate of the conductance of sediments, filling the graben. In order to explain the observed Rhine graben anomaly of geomagnetic variations between 0.5 and 6 cycles/hour, a stratified conducting substratum has to be added with a layer of high conductivity ($0.03\ \Omega^{-1}\mathrm{m}^{-1}$) between 25 and 75 km depth. Concurrent magneto-telluric observations between 4 and 400 cycles/hour by Scheelke (1972)

support this interpretation.

In conclusion it may be interesting to note that the original model distributions "d" and "e", which Lahiri and Price (1939) derived from global studies for the earth as a whole, involved an outermost shell of high conductance, enclosing a poorly conducting intermediate zone with a highly conducting core. This surface shell was necessary to explain the internal part of D_{st} and S_q with one model.

Lahiri and Price saw in its necessity the smoothed-out effect of the oceans, but pointed out that a highly conducting layer at some depth beneath the surface could be the cause also. In exploring new evidence for this intermediate layer of high conductivity global and regional studies meet and we may expect that their sometimes conflicting results will eventally merge into a unified concept about the deep distribution of electrical conductivity beneath continents and oceans.

References

Adam, A., 1970. *J. Geomagn. Geoelectr.*, 22: 223.

Barsczus, H.G., 1970. *Sondages géomagnétiques bibliographies.* Orstom, Paris, 84pp.

Berdichevskij, M.N., Borisova V.P., Van'yan, L.L., Feldman, I.S. and Yakovlev, I.A., 1969. *Izv. Akad. Nauk S.S.S.R., Ser. Fiz. Zemli,* 10: 43.

Camfield, P.A. and Gough, D.I., 1973. *J. Geophys. Res.*, in press.

Camfield, P.A., Gough, D.I. and Porath, H., 1970. *Geophys. J.*, 22: 201.

Caner, B., 1971. *J. Geophys. Res.*, 76: 7202.

Caner, B., Camfield, P.A., Andersen, F. and Niblett, E.R., 1969. *Can. J. Earth Sci.*, 6: 1245.

Caner, B., Auld, D.R., Drägert, H. and Camfield, P.A., 1971. *J. Geophys. Res.*, 76: 7181.

Cox, C.S., 1971. The electrical conductivity of the oceanic lithosphere. In: J.G. Heacock (Editor), *The Structure and Physical Properties of the Earth's Crust.* American Geophysical Union, Washington, D.C., p. 227.

Dowling, F.L., 1970. *J. Geophys. Res.*, 75: 2683.

Edwards, R.N., Law, K.L., and White, A., 1971. *Philos. Trans. R. Soc. Lond., Ser. A,* 270: 289.

Filloux, J., 1967. *Oceanic Electric Currents, Geomagnetic Variations and the Deep Electrical Conductivity Structure of the Ocean–Continent Transition of Central California.* Thesis, Univ. California, San Diego, Calif.

Fournier, H., 1969. *Ensayo historico sobre los conocimientos Magnetoteluricos.* Observatoria del Ebro, Roquetas/ Tarragona, 320pp.

Fournier, H., 1970, *Contribution au developpement de la méthode magnétotellurique,* Thèse, Univ. Paris.

Grafe, A., 1964. *Abh. 31 Dtsch Akad. Wiss, Geomagn. Inst, Potsdam.* Akademie Verlag, Berlin.

Greenhouse, J.P., 1972. *Geomagnetic Time Variations on the Sea Floor off southern California.* Thesis, Univ. California, San Diego, Calif.

Haak, V., 1970. *Das zeitlich sich ändernde, erdelektrische Feld, beobachtet auf einem Profil über den Rheingraben,* Dissertation Univ.München.

Hermance, J.F. and Grillot, L.R., 1970. *J. Geophys. Res.*, 75: 6582.

Hermance, J.F. and Peltier, W.R., 1970. *J. Geophys. Res.*, 75: 3351.

Hobbs, B.A., 1971. *Geophys. J.*, 25: 481.

Hobbs, B.A., and Price, A.T., 1970. *Geophys. J.*, 20: 49.

Hutton, R., 1972. *Geophys. J.*, 28: 267.

Hutton, R. and Leggeat, A., 1972. *Geophys. J.*, 28: 411.

Hyndman, R.D. and Cochrane, N.A., 1971. *Geophys. J.*, 25: 425.

Klein, D.P., 1972. *Geomagnetic Time-Variations, the Island Effect, and Electromagnetic Depth Sounding on Oceanic Island.* Thesis, Univ. Hawaii.

Lahiri, B.N. and Price, A.T., 1939. *Philos. Trans. R. Soc. Lond., Ser. A,* 237: 509.

Larsen, J. and Cox, C., 1966. *J. Geophys. Res.*, 71: 4441.

Madden, T.R. and Swift, C.M., 1969. Magnetotelluric studies of the electrical conductivity of the crust and upper mantle. In: P.J. Hart (Editor), *The Earth's Crust and Upper Mantle.* American Geophysical Union, Washington, D.C., p.469.

Meyer, J., 1966. *Gerlands Beitr. Geophys.*, 75: 289.

Mitchell, B.J. and Landisman, M., 1971. *Geophysics,* 36: 363.

Moses, R., Elvers, D. and Perkins, D., 1966. *A Reconnaissance of Conductivity Effects in the United States.* U.S. Coast and Geodet. Survey, Washington, D.C., unpublished.

Niblett, E.R. and Witham, K., 1970. *J. Geomagn. Geoelectr.*, 22: 99.

Oni, E. and Alabi, A.O., 1972. *Phys. Earth Planet. Inter.*, 5: 179.

Parkinson, W.D., 1971. *Gerlands Beitr. Geophys.*, 80: 199.

Porath, H. and Dziewonski, A., 1971a. *Geophysics,* 36: 382.

Porath, H. and Dziewonski, A., 1971b. *Rev. Geophys. Space Phys.*, 9: 891.

Porath, H., Gough, D.I. and Camfield, P.A., 1971. *Geophys. J.*, 23: 387.

Rikitake, T., 1971. *Earth Sci. Rev.*, 7: 35.

Rokitjanskij, I.I., Logvinov, I.M. and Luginina, N.A., 1969. *Izv. Akad. Nauk S.S.S.R., Ser. Fiz. Zemli,* 3: 100.

Rooney, W., 1935. *Terr. Magn.*, 40: 183.

Scheelke, I., 1972. *Magnetotellurische Messungen im Rheingraben und ihre Deutung mit zweidimensionalen Modellen.* Dissertation, Univ. Braunschweig.

Schmidt, H., 1968. *Gerlands Beitr. Geophys.*, 77: 50.

Schmucker, U., 1970a. Anomalies of geomagnetic variations in the southwestern United States. *Bull. Scripps Inst. Oceanogr. Univ. Calif.*, 13: 165.

Schmucker, U., 1970b. *J. Geomagn. Geoelectr.*, 22: 9.
Schmucker, U., 1971. *Geophysics*, 36: 156.
Schmucker, U. and Jankowski, J., 1972. *Tectonophysics*, 13: 233.
Schmucker, U., Hartmann, O., Giesecke, A.A., Casaverde, M. and Forbush, S.E., 1964. *Carnegie Inst. Wash., Yearbook*, 63: 354.
Shneyer, V.S., 1971. *Geomagn. Aeron.*, 11: 308.
Shneyer, V.S. and Fonarev, G.A., 1968. *Geomagn. Aeron.*, 8: 479.
Siebert, M. and Kertz, W., 1957. *Nachr. Akad. Wiss. Göttingen, Math.-Phys. Kl., Abt. IIa*, No.5: 87.
Srivastava, S.P., 1971. *Earth Planet. Sci. Lett.*, 10: 423.
Srivastava, S.P., and White, A., 1971. *Can. J. Earth Sci.*, 8: 204.
Vozoff, K., 1972. *Geophysics*, 37: 98.
Weidelt, P., 1972. *Z. Geophys.*, 38: 257.
Winter, R., 1973. Electromagnetic induction studies in the Rhinegraben area. A model for the resistivity distribution from geomagnetic depth soundings. In: H. Illies and K. Fuchs (Editors), *Approaches to Taphrogenesis*. Schweizerbart, Stuttgart, in press.